

An integer linear programming model for efficient scheduling of UGV tasks in precision agriculture under human supervision

Original

An integer linear programming model for efficient scheduling of UGV tasks in precision agriculture under human supervision / FOTIO TIOTSOP, Lohic; Servetti, Antonio; Masala, Enrico. - In: COMPUTERS & OPERATIONS RESEARCH. - ISSN 0305-0548. - STAMPA. - 114:(2020). [10.1016/j.cor.2019.104826]

Availability:

This version is available at: 11583/2764434 since: 2020-07-15T22:08:40Z

Publisher:

Elsevier

Published

DOI:10.1016/j.cor.2019.104826

Terms of use:

This article is made available under terms and conditions as specified in the corresponding bibliographic description in the repository

Publisher copyright

Elsevier postprint/Author's Accepted Manuscript

© 2020. This manuscript version is made available under the CC-BY-NC-ND 4.0 license
<http://creativecommons.org/licenses/by-nc-nd/4.0/>. The final authenticated version is available online at:
<http://dx.doi.org/10.1016/j.cor.2019.104826>

(Article begins on next page)

An Integer Linear Programming Model for Efficient Scheduling of UGV Tasks in Precision Agriculture under Human Supervision

Lohic Fotio Tiotsop, Antonio Servetti, Enrico Masala

*Control and Computer Engineering Department
Politecnico di Torino
Corso Duca degli Abruzzi 24, 10129 Torino, Italy*

Abstract

In precision agriculture more and more robots are being used to perform tasks that may include some farming activities, such as pruning, inspection or spraying, assigned to the robot as a result of a previous analysis activity or autonomously identified by the machine itself. In this sensitive scenario, reporting difficult situations to a decision maker, e.g., a human operator or some sophisticated software tools that cannot be integrated with the robot, could be useful to perform the correct action that the machine has to execute. Unfortunately, this key aspect is still neglected in current literature that focuses, instead, on fully automated operations by robots. Moreover, it is necessary to consider that in rural areas it often happens that successful data communication can only be achieved in certain locations in the field. In this context, we aim to address all the previous shortcomings by formulating a more comprehensive optimization problem, which also models the necessity to report to a central location and get instructions on the task to be done before proceeding to perform each action. After presenting two alternative analytical formulations of the problem, i.e. an integer linear programming model (ILP) and a mixed integer linear programming model, we propose a branch and bound algorithm that is guaranteed to find the global minimum cost solution in terms of navigation time. Simulation

Email address: lohic.fotiotiotsop@polito.it, antonio.servetti@polito.it, enrico.masala@polito.it (Lohic Fotio Tiotsop, Antonio Servetti, Enrico Masala)

results show that our proposed algorithm performs about 20 to 30 times faster with respect to commercial linear programming solvers using any of the two analytical models proposed. Moreover, we also propose further improvements to reduce computational time while maintaining solution optimality. Finally, some insight into the development of future heuristics is given by analyzing the speed of convergence towards the optimal solution.

Keywords: data acquisition, farming activities, UGV navigation, integer linear programming, service robotics

1 Introduction

The amount of robots employed in agriculture applications is constantly increasing. Two types of robots are typically used: unmanned ground vehicles (UGV) and unmanned aerial vehicles (UAV) [1]. Examples are rovers that navigate the cultivation to perform specific agriculture tasks, e.g., inspection or physical operations such as collecting samples, pruning, spraying [2]. UAVs, instead, are mainly used for imagery tasks, i.e., to take pictures for later processing in order to understand the status and requirements of different parts of the cultivation [3, 4]. Collaboration between UAVs and UGVs is also being actively explored [5, 6].

Despite some operations can be done autonomously by the robots, sometimes communication with a central location is needed, so that a human operator or an algorithm, more sophisticated compared to the one that can run on the robot, can be used in the loop to take decisions and act accordingly in a specific terrain position. In fact, a recent survey about the usage of agricultural robots [7] pointed out the lack of models considering such aspect in the current literature, while at the same time highlighting its necessity to correctly model actual problems.

Note that this work relies on an agricultural scenario to present the models just because it seems to be one of the most challenging real applications, but it can also cover other real situations, such as the one described in the follow-

22 ing. In case of industrial operations being performed by robots with human
23 supervision, there could be A (A typically large) jobs located in different places
24 to be performed by a robot and a supervisor operator may just have a rough
25 knowledge of what is the exact job to be done at each location. There are also B
26 locations where the robots can collect what is needed to perform a job. The pro-
27 posed models can be used to schedule the A jobs minimizing the time required
28 to complete them. At any job location the robot first performs an inspection,
29 then moves to a point of type B , if necessary, by sending in the meanwhile a
30 report to the supervisor operator that decides what to do and what is needed
31 to perform the job and informs the robots that then act accordingly. Another
32 example is repair companies: they may rely on the proposed models to sched-
33 ule their logistic operations. The customer locations would represent points of
34 interests and the company warehouses are the points to be visited to perform
35 repairs at the point of interests. More precisely, when an operator leaves the
36 main warehouse in the morning, at each customer location he/she either fixes
37 the problem (if the description was exhaustive) or collects information about
38 the problem and what is needed, then visits a company warehouse in order
39 to pick up all he needs and go back later to the customer location to fix the
40 problem. More in general, our models can be used for efficiently planning oper-
41 ations requiring data acquisition, data elaboration or transmission, and finally
42 an action.

43 In this work we focus on the specific agriculture scenario considering and
44 modelling the constraint imposed by communicating with a decision maker,
45 e.g., a human operator, before performing physical actions. Considering the
46 optimization problem, we assume to have a rough preliminary knowledge about
47 the terrain and how a UGV can move in the area. In other words, obstacle
48 positions and possible navigation paths are known. This can be obtained by
49 previous knowledge or by means of a survey, e.g., made using a UAV or other
50 similar technologies. During the survey, points of interests (POIs) are also
51 identified, i.e., areas to be visited by the UGV in order to gather information,
52 decide what to do and act accordingly. Since the decision of the action to

53 perform in each POI might be difficult to take only relying on the on-board
54 processing capabilities or simply might require human judgment not available
55 through algorithms, we assume that after the UGV has gathered information
56 by moving to the POI and taking, e.g., a picture, it must communicate with
57 a central location to get an answer about the farming action to perform. The
58 UGV must then perform the action returning to the POI, if necessary.

59 However, it is well known that communications, including wireless, in rural
60 areas might be difficult [8], mainly due to two reasons. The first reason is,
61 sometimes, the presence of massive physical constraints, such as hills, rocks,
62 subsidence [9]. The second reason is the typically scarce coverage of 3G/4G
63 cellular technology, since there is small incentive for network operators to pro-
64 vide good quality coverage of such areas due to, e.g., the low people density. As
65 a consequence, depending on the physical position, either no communication is
66 possible or only wireless communications are available but with locally-deployed
67 infrastructure such as Wi-Fi access points or similar systems, potentially tuned
68 to communicate over longer distance compared to the usual home devices. In
69 our scenario, we assume that we roughly know that in certain places on the
70 terrain communication is possible, whereas in others this is not possible at all.
71 Such information could come as a result of a previous survey, or considering the
72 relative position of the devices, the terrain topography and similar features.

73 Our goal is to provide an efficient algorithm to solve the navigation problem
74 of the UGV on the terrain while minimizing the time needed to perform all the
75 tasks in the previously determined POIs, considering that before performing a
76 task in a POI it has to i) visit the POI and collect some data about its state,
77 ii) visit a location where those data can be transmitted and instructions on
78 the task to be done are received, iii) go to the POI and perform the action.
79 Obviously the UGV does not have to perform the three steps sequentially for
80 each POI, but it can visit multiple POIs before moving to a place where it
81 can communicate, and then it can go back to each one of them, in any order,
82 to execute the received instructions. Minimizing the time taken by the UGV is
83 economically advantageous for many reasons. For instance, if the UGV is rented,

84 it can operate in more places therefore serving more than one customer, thus
85 the company renting it can maximize its earnings. Conversely, if the UGV needs
86 to be bought, a lower number of them is needed to perform all the activities
87 in the timeframe required by the specific agriculture scenario so that the UGV
88 could potentially be employed for other activities.

89 This paper significantly extends our preliminary work [10]. In particular,
90 we present an improved version of our proposed branch and bound algorithm
91 which relies on the computation of a lower bound to reduce the execution time.
92 Moreover, an additional mixed ILP model employing dummy vertices is pre-
93 sented for comparison purposes. Finally, this paper includes an extensive set
94 of performance results on several different graph instances, i.e. fifty instances
95 for each level of complexity, both using the two ILP models and the proposed
96 algorithm.

97 The paper is organized as follows. Section 2 reviews related work in the
98 field, whereas Section 3 explains how to represent the graph which is the basic
99 input data for our algorithm. Then, the optimization problem is analytically
100 formulated in Section 4 as two ILP problems, using two different approaches, to
101 study its characteristics. In Section 5 a specific algorithm for the problem is de-
102 signed and implemented in the form of a branch and bound algorithm, and some
103 efficient pruning and lower bounding strategies are proposed. Section 6 shows
104 some practical experimental results on realistic graphs, followed by conclusions
105 in Section 7.

106 **2. Related work**

107 Sensing technologies are more and more used in agricultural applications to
108 perform crop monitoring [11, 12]. For instance, imaging sensors in the visible
109 spectrum [13] or at other wavelengths [14] are often used. Image data can then
110 be elaborated to detect cultivation type, e.g., vineyard [15], or to detect single
111 plants and potential anomalies [16]. A more comprehensive overview of such
112 technologies can be found in [17].

113 Potential issues can be identified and transformed into a set of POIs so that,
114 on the basis of the cultivation map, a UGV can move in such positions in order
115 to perform a more detailed analysis, e.g., taking closer pictures or perform local
116 measures with sensors, to later perform some specific physical action [18, 19].
117 For the purpose of solving the UGV movement problem, the cultivation field
118 can be abstracted in the form of a graph with nodes (i.e., the POIs) connected
119 by edges whose weight represent the cost, in terms of time, needed to move from
120 one point to the other.

121 Graph visiting problems have been well investigated from the theoretical
122 point of view. The travelling salesman problem (TSP) or more in general the
123 vehicle routing problem (VRP) and some variants have been intensively studied
124 in literature [20, 21, 22, 23, 24, 25]. In short, they consider a set of vehicles
125 that can transport goods and a graph whose nodes represent a set of customers,
126 each one characterized by a given demand. Each edge represents the cost that
127 should be sustained to move from a customer to another. The VRP aims at
128 determining which customers should be served by any vehicle and the schedule
129 of the operations of any vehicle in order to minimize the total cost satisfying
130 the capacity constraint of each vehicle and the demand of each customer. In
131 case of a single vehicle, the problem is reduced to the TSP.

132 Reducing field work time in agriculture by optimally scheduling agricultural
133 tasks is often assimilated in the literature to graph visiting problem. In [26,
134 27, 28] the authors explain how the VRP can be used to gain efficiency in field
135 logistics. In particular in [26] the numerical experiments show that it is possible
136 to save up to 32% of the time if the operations are guided by the solution of
137 the proposed VRP instead of an intuitive approach. The TSP is used in [29] to
138 schedule the farming activities in fields characterized by the presence of a large
139 number of obstacles.

140 While the goal of these works is to minimize the time needed to complete
141 the assigned farming tasks, similarly to our navigation problem, nevertheless
142 they are substantially different in the fact that they do not consider the com-
143 munication aspect and thus the interaction with an external decision maker,

144 e.g., a human operator or any other external tool, whose presence coordinates
145 the operations and addresses critical situations.

146 Some VRP variants are somehow more similar to our case, for instance the
147 so called vehicle routing problem with intermediate stops (VRP-IS) [30]. An
148 intermediate stop (IS) is a stop that occurs at a node whose visit is neces-
149 sary to keep the vehicle operational or to perform any other action necessary
150 to pursuit the main task assigned to the vehicle. ISs have been considered
151 for replenishment [31], unloading of waste [32], refueling [33, 34], rest [35] and
152 synchronization requirements [36]. Similarly to the VRP-IS, our problem con-
153 siders, besides the POIs where physical actions are required, the points covered
154 by wireless network where the UGV might stop to transfer the data collected
155 until that point and get instructions about the correct actions to perform later
156 at the POIs. In our problem the UGV is hence constrained to visit each POIs
157 again once the data acquired during the first visit have been transmitted. This
158 clearly introduces further constraints compared to the cited works.

159 The more practical problem of computing the exact physical path corre-
160 sponding to each edge in our graph is addressed in the robotics research field
161 by works focusing on robot navigation problems. For instance, one of the most
162 common problems is the so-called path-planning, in which a trajectory must be
163 computed so that a robot can move to a certain target position while fulfilling
164 certain constraints, i.e., avoiding obstacles and forbidden or dangerous condi-
165 tions [37, 38, 39]. More complex constraints can be taken into account, e.g., the
166 slope of the terrain, as in [40] that presents the case of a UGV that needs to
167 visit all the rows in a vineyard.

168 Once edge weights and node positions are known, our problem resembles
169 (but it is not the same) the Steiner TSP (STSP) [41]. Given a graph, a cost for
170 each edge of the graph and a subset of nodes that represent customers, the STSP
171 aims at finding the minimum-cost tour that passes through each customer node.
172 Edges may be traversed more than once, and nodes visited more than once, if
173 necessary. Such a problem, despite being somehow similar to ours, presents an
174 important difference. In that problem, all clients have to be visited at least

175 once. In ours, we require to visit at least *twice* the POI nodes making sure that
176 at least one of the visits at a given POI occurs *after* the transmission of the
177 related information. This further increases the complexity, since time variables
178 need to be introduced in order to manage the chronology of the tasks.

179 **3. Graph representation**

180 In our work we assume that a picture has been used to derive a graph that
181 represents the field in which the UGV must operate. The task of creating a
182 graph from a picture by detecting the different types of areas and how they are
183 connected and which is the optimal movement path between different areas is
184 a problem well addressed in literature (see [42, 43, 44, 45]). Therefore, here
185 we assume that such a graph is available. In more details, in our scenario
186 the graph includes nodes, which correspond to physical locations in the terrain.
187 Such nodes are connected with edges whose weight represents the cost of moving
188 from one node to the other. Obstacles and possible movement paths are already
189 modeled in such weights.

190 Concerning nodes, they can be classified into three types.

- 191 • Type A: The nodes that we want to visit, in which a physical operation
192 has to be performed by the robot.
- 193 • Type B: The nodes in which we are sure that wireless communication
194 can be established in order to both transmit the information collected
195 at previous ‘A’ nodes and receive instructions about what to do in those
196 nodes.
- 197 • Type AB: The nodes with the characteristics of both ‘A’ and ‘B’. When
198 visited, the physical operation can be immediately performed after data
199 communication has taken place, since it is possible to immediately com-
200 municate and receive instructions.

201 Detecting ‘A’ nodes heavily depends on the specific task to do (e.g., detecting
202 potential weeds, or places where plant pruning operations might be necessary).

203 The same applies for ‘B’ nodes, in which wireless communication models, com-
 204 bined with the terrain geography can be used to determine the possible coverage,
 205 or maybe the information is simply available from a previous survey.

206 4. Mathematical formulations

207 In this section two alternative models of the problem are presented. Both
 208 models need to address the problem of modeling the movements of the UGV
 209 that needs to traverse nodes and edges an unknown number of times. The first
 210 formulation addresses the issue by means of an ordered set of displacements (i.e.,
 211 a movement from a node to another) that the UGV must follow to complete
 212 the required tasks. In this formulation the UGV can pass more than one time
 213 on the same node, whereas in the second model this condition is considered by
 214 means of dummy vertices (i.e., replica nodes to consider multiple visits).

215 4.1. Displacement-based formulation (Model I)

216 Let us define the following elements:

- 217 • \mathcal{A} : the set of nodes to visit (Type ‘A’ or ‘AB’)
- 218 • \mathcal{B} : the set of nodes where wireless communication can be established (Type
 219 ‘B’ or ‘AB’)
- 220 • $\mathcal{V} = \mathcal{A} \cup \mathcal{B}$ set of all nodes
- 221 • \mathcal{K} : the set of displacements of the UGV
- 222 • \mathcal{E} : the set of edges connecting the different nodes
- 223 • A, B, E and K respectively the cardinality of $\mathcal{A}, \mathcal{B}, \mathcal{E}$ and \mathcal{K}
- 224 • s the depot node or the central location
- 225 • t_{ij} : the time required to cover the edge $(i, j) \in \mathcal{E}$
- 226 • x_{ij}^k : a boolean variable equal to 1 if during its k -th displacement the UGV
 227 moves along the edge $(i, j) \in \mathcal{E}$

- 228 • y_i^k : a boolean variable equal to 1 if during the k -th displacement the UGV
 229 transfers the data collected from the node $i \in \mathcal{A}$

The problem is formulated as follows

$$\min_{x,y} \sum_{k \in \mathcal{K}} \sum_{(i,j) \in \mathcal{E}} x_{ij}^k t_{ij} \quad (1)$$

230 st:

$$\sum_{\{j \in \mathcal{A} \cup \mathcal{B} : (s,j) \in \mathcal{E}\}} x_{sj}^1 = \sum_{\{i \in \mathcal{A} \cup \mathcal{B} : (i,s) \in \mathcal{E}\}} x_{is}^K = 1, \quad (2)$$

$$\sum_{(i,j) \in \mathcal{E}} x_{ij}^k = 1 \quad \forall k \in \mathcal{K}, \quad (3)$$

$$\sum_{k \in \mathcal{K}} y_i^k = 1 \quad \forall i \in \mathcal{A}, \quad (4)$$

$$\sum_{k \in \mathcal{K}} \sum_{\{i \in \mathcal{A} \cup \mathcal{B} : (i,j) \in \mathcal{E}\}} x_{ij}^k \geq \begin{cases} 2 & \forall j \in \mathcal{A} \setminus \mathcal{B}, \\ 1 & \forall j \in \mathcal{A} \cap \mathcal{B}, \end{cases} \quad (5)$$

$$x_{ij}^{k-1} \leq \sum_{\{i \in \mathcal{A} \cup \mathcal{B} : (j,i) \in \mathcal{E}\}} x_{ji}^k \quad \forall (i,j) \in \mathcal{E} \quad \forall k \in (\mathcal{K} \setminus \{1\}), \quad (6)$$

$$y_i^k \leq \sum_{\{j \in \mathcal{B} : (i,j) \in \mathcal{E}\}} x_{ij}^k \quad \forall i \in \mathcal{A} \quad \forall k \in \mathcal{K}, \quad (7)$$

$$y_j^k \leq \sum_{1 \leq t \leq k} \sum_{\{i \in \mathcal{A} \cup \mathcal{B} : (i,j) \in \mathcal{E}\}} x_{ij}^t \quad \forall j \in \mathcal{A} \quad \forall k \in \mathcal{K}, \quad (8)$$

$$y_j^k \leq \begin{cases} \sum_{k+1 \leq t \leq K} \sum_{\{i \in \mathcal{A} \cup \mathcal{B} : (i,j) \in \mathcal{E}\}} x_{ij}^t & \forall j \in \mathcal{A} \setminus \mathcal{B} \quad \forall k \in \mathcal{K} \setminus \{K\}, \\ 0 & \forall j \in \mathcal{A} \setminus \mathcal{B}, k = K \end{cases} \quad (9)$$

$$x_{ij}^k \in \{0, 1\} \quad \forall (i,j) \in \mathcal{E} \quad \forall k \in \mathcal{K}, \quad (10)$$

$$y_i^k \in \{0, 1\} \quad \forall i \in \mathcal{A} \quad \forall k \in \mathcal{K}, \quad (11)$$

231 Eq. (1) requires the minimization of the total time required to perform all
 232 the operations, Eq. (2) imposes that the path of the UGV should start and
 233 end at the depot. The constraints in Eq. (3) ensure that each displacement
 234 of the UGV corresponds to one edge in the solution and Eq. (4) requires that
 235 the data collected from any node $i \in \mathcal{A}$ are transmitted once and only once.
 236 The constraints in Eq. (5) ensure that the UGV visits, i) at least twice, the
 237 nodes of interest in the set $\mathcal{A} \setminus \mathcal{B}$ where it is not possible to communicate and
 238 ii) at least once, the other nodes of interest in the set $\mathcal{A} \cap \mathcal{B}$. Eq. (6) are flow
 239 conservation constraints. The fact that the UGV might transfer from a node
 240 only if such node belongs to the set \mathcal{B} is given by Eq. (7). Eq. (8) requires that
 241 the UGV transfers the information related to a given node in the set \mathcal{A} only if
 242 such node has already been visited, Eq.(9) requires that, once the information
 243 corresponding to the visit of a node in the set $\mathcal{A} \setminus \mathcal{B}$ where communication is not
 244 possible has been transmitted, the UGV must visit the node again once more.
 245 Finally Eq. (10) and Eq. (11) ensures that the variables of the optimization
 246 problem have a binary value.

247 One of the main reason of the complexity of the problem in Eq. (1)-(11) is
 248 that it includes the parameter K whose value is unknown a priori. K actually
 249 represents the number of displacements the UGV needs to perform before com-
 250 pleting the required tasks. This issue could be solved by assigning a very large
 251 value to K and allowing the UGV not to move to a new node to match the K
 252 value. Unfortunately, the number of binary variables in the problem increases
 253 with K , therefore the complexity of the problem easily increases. On the other
 254 hand, if the value of K is underestimated the problem might become infeasible or
 255 the model may lead to a feasible solution that is not the optimal one. Another
 256 alternative to tackle such difficulty could be the column generation approach
 257 (CGA) whose implementation requires to formulate a restrictive master prob-
 258 lem (RMP) associated with the problem in Eq. (1)-(11) and progressively add
 259 new columns and thus new variables to the RMP until the minimum number of
 260 variables necessary to get the optimal solution is reached. More details about
 261 the CGA can be found in [46, 47]. The main drawback of this approach is the

262 difficulty of getting a RMP associated with a given integer linear programming
 263 problem that guarantees both the effectiveness and the efficiency of the CGA.

264 The minimum value for K needed to obtain the optimal solution is strongly
 265 related to the topology of the underlying graph of the problem, nevertheless the
 266 following proposition holds:

267 **Proposition 4.1.** *Let L denote the number of edges that constitutes the short-
 268 est path between a pair of nodes in \mathcal{V} having the largest number of edges and AB
 269 the cardinality of $\mathcal{A} \cap \mathcal{B}$. If $K \geq L(3A - 2AB + 1)$ then the solution provided by
 270 the model in Eq. (1)-(11) is the optimal one.*

271 *Proof* First, consider the case in which the graph is complete and thus $L = 1$.
 272 Denoting by N_i the total number of times the UGV visits and leaves a node
 273 $i \in \mathcal{V}$ before any solution is found, it follows that

$$274 \quad \sum_{i \in \mathcal{V}} N_i = 2K. \quad (12)$$

275 Since each node $a \in \mathcal{A} \setminus \mathcal{B}$ has to be visited twice and that since the graph is
 276 complete, extra visits cannot occur in a , therefore

$$277 \quad N_a = 4. \quad (13)$$

278 Furthermore, a node $b \in \mathcal{B}$ is visited to transmit the data collected at one or
 279 more nodes $a \in \mathcal{A}$, hence

$$280 \quad \sum_{b \in \mathcal{B}} N_b \leq 2A. \quad (14)$$

281 Using (13) and (14) and considering that the UGV needs to leave the depot s
 282 and return back there at the end of the tour (thus 2 more displacements are to
 283 be added to N_s):

$$284 \quad 2K = \sum_{i \in \mathcal{V}} N_i = \sum_{a \in \mathcal{A} \setminus \mathcal{B}} N_a + \sum_{b \in \mathcal{B}} N_b \leq 4(A - AB) + 2A + 2 = 6A - 4AB + 2$$

285 Hence if $K \geq 3A - 2AB + 1$ any feasible solution will be explored. In the more
 286 general case in which the graph is connected but not complete, extra visits to
 287 a given node than those needed for data collection, transmission or to perform

288 some action are expected to occur. For instance the UGV might move from a B
 289 node to another B node to reach an A node. By definition of L , any operation
 290 requiring a single displacement, when the graph is complete, can be performed
 291 after at most L displacements of the UGV in case the graph is connected but
 292 not complete. Hence, all the feasible solutions will be examined if

$$293 \quad K \geq L(3A - 2AB + 1). \quad (15)$$

294

295 4.2. Dummy-Vertices-Based formulation (Model II)

296 In this section, we explore an alternative formulation of the problem. Fol-
 297 lowing the approach of [34] we use the so-called dummy vertices to take into
 298 account that vertices can be visited more than once. Let us define the following
 299 elements:

- 300 • d the number of dummy replications of each vertex
- 301 • \mathcal{V}_d set of all vertices including the dummy vertices
- 302 • \mathcal{E}_d set of all edges including the dummy edges
- 303 • $\mathcal{D}_i = \{i_1, i_2, \dots, i_d\}$ set of the d dummy vertices associated with the vertex
 304 $i \in \mathcal{V}$, e.g., s_1 and s_d are respectively the first and the last dummy vertex
 305 associated to the depot s
- 306 • $x_{ij}=1$ if the arc $(i, j) \in \mathcal{E}_d$ is in the solution and 0 otherwise
- 307 • τ_i the time at which the vertex $i \in \mathcal{V}_d$ is visited
- 308 • $y_{ij} = 0$ if $\tau_j \notin [\tau_{i_1}, \tau_{i_d}] \quad \forall i \in \mathcal{A} \setminus \mathcal{B}, j \in \mathcal{B}_d$
- 309 • $T = d \sum_{(i,j) \in \mathcal{E}} t_{ij}$

The problem can then be alternatively formulated as follows:

$$\min_{x,y} \sum_{(i,j) \in \mathcal{E}_d} x_{ij} t_{ij} \quad (16)$$

$$\sum_{i \in \mathcal{V}_d, (i,j) \in \mathcal{E}_d} x_{ij} \leq 1 \quad \forall j \in \mathcal{V}_d \quad (17)$$

$$\sum_{j \in \mathcal{V}_d, (i,j) \in \mathcal{E}_d} x_{ij} - \sum_{j \in \mathcal{V}_d, (i,j) \in \mathcal{E}_d} x_{ji} = 0 \quad \forall i \in \mathcal{V}_d, i \neq s_1, i \neq s_d \quad (18)$$

$$\sum_{i \in \mathcal{V}_d, (i,j) \in \mathcal{E}_d} x_{ij} \geq 1 \quad \forall j \in \mathcal{A} \cap \mathcal{B} \quad (19)$$

$$\sum_{j \in \mathcal{V}_d, (j,i_1) \in \mathcal{E}_d} x_{ji_1} \geq 1 \quad \forall i \in \mathcal{A} \setminus \mathcal{B} \quad (20)$$

$$\sum_{j \in \mathcal{V}_d, (j,i_d) \in \mathcal{E}_d} x_{ji_d} \geq 1 \quad \forall i \in \mathcal{A} \setminus \mathcal{B} \quad (21)$$

$$\tau_{i_k} + T \left(1 - \sum_{j \in \mathcal{V}_d, (j,i) \in \mathcal{E}_d} x_{ji_k} \right) \geq \tau_{i_1} \quad \forall i \in \mathcal{A} \setminus \mathcal{B}, k = 1, 2, \dots, d \quad (22)$$

$$\tau_{i_k} - T \left(1 - \sum_{j \in \mathcal{V}_d, (j,i) \in \mathcal{E}_d} x_{ji_k} \right) \leq \tau_{i_d} \quad \forall i \in \mathcal{A} \setminus \mathcal{B}, k = 1, 2, \dots, d \quad (23)$$

$$\sum_{j \in \mathcal{B}_d} y_{ij} \geq 1 \quad \forall i \in \mathcal{A} \setminus \mathcal{B} \quad (24)$$

$$\sum_{i \in \mathcal{V}_d, (i,j) \in \mathcal{E}_d} x_{ij} \geq y_{kj} \quad \forall j \in \mathcal{B}_d, k \in \mathcal{A} \setminus \mathcal{B} \quad (25)$$

$$\tau_{i_1} - T(1 - y_{ij}) \leq \tau_j \leq \tau_{i_d} + T(1 - y_{ij}) \quad i \in \mathcal{A} \setminus \mathcal{B}, j \in \mathcal{B}_d \quad (26)$$

$$\tau_i + t_{ij}x_{ij} - T(1 - x_{ij}) \leq \tau_j \quad (i, j) \in \mathcal{E}_d \quad (27)$$

$$\sum_{j \in \mathcal{V}_d, (j,s_1) \in \mathcal{E}_d} x_{s_1j} = 1 \quad (28)$$

$$\sum_{j \in \mathcal{V}_d, (j, s_d) \in \mathcal{E}_d} x_{js_d} = 1 \quad (29)$$

$$\tau_{s_1} - T \left(1 - \sum_{i \in \mathcal{V}_d, (i, j) \in \mathcal{E}_d} x_{ij} \right) \leq \tau_j \leq \tau_{s_d} + T \left(1 - \sum_{i \in \mathcal{V}_d, (i, j) \in \mathcal{E}_d} x_{ij} \right) \quad (30)$$

$$j \in \mathcal{V}_d, j \neq s_1, j \neq s_d$$

$$x_{ij} \in \{0, 1\} \quad (i, j) \in \mathcal{E}_d \quad (31)$$

$$y_{ij} \in \{0, 1\} \quad i \in \mathcal{A} \setminus \mathcal{B}, j \in \mathcal{B}_d \quad (32)$$

$$\tau_i \in [0, +\infty) \quad i \in \mathcal{V}_d \quad (33)$$

311 The model can be interpreted as follows. The minimization of the time
 312 required to complete the tour is expressed in (16). The constraints (17) state
 313 that any dummy node should be visited at most once. Constraints (18) establish
 314 flow conservation by requiring that the number of incoming arcs of each node
 315 (except the vertices s_1 and s_d) is equal to the outgoing ones. Constraints (19)
 316 enforce that each node of type AB is visited at least once. The constraints (20)-
 317 (23) handle the two visits needed in each node of type A where data transmission
 318 is not allowed. In fact $\forall i \in \mathcal{A} \setminus \mathcal{B}$ it is required that the associated dummy nodes
 319 i_1 and i_d should be visited. Furthermore, the first and the last visit in i should
 320 occur using respectively i_1 and i_d . Constraints (24)-(25) ensure that the data
 321 collected in each node $i \in \mathcal{A} \setminus \mathcal{B}$ are transmitted from some node $j \in \mathcal{B}_d$ before the
 322 last visit to node i occurs, while (26) models the relation between the variables
 323 y_{ij} , τ_j , τ_{i_1} , τ_{i_d} . Time constraints are expressed in (27). The constraints (28)-
 324 (29) enforce the connectivity between the starting location and the other nodes.
 325 Constraints (30) require that the tour starts and ends at the depot s . Finally,
 326 (31)-(33) determine the domain of the decision variables.

327 **5. Proposed solution**

328 To avoid an unreasonable increase in the number of decision variables, we
 329 propose to employ a graph visiting algorithm coupled with a branch and bound
 330 approach so that all possible solutions are explored while complexity is mini-
 331 mized. For the sake of convenience we remind the goal of the problem. Starting
 332 from the depot s , the UGV must visit every node $a \in \mathcal{A}$, acquire some data,
 333 find a location $b \in \mathcal{B}$ where the data can be sent, receive instructions, go back
 334 to a , perform the required task and, at the end, return back to s spending the
 335 lowest possible amount of time.

336 Let us denote by a_1, a_2, \dots, a_A the A nodes to be visited. While the UGV is
 337 moving through the graph, the state of the UGV itself is completely defined by

338
$$\mathbb{S} = (n_1, n_2, \dots, n_A, u, c)$$

339 where u is the node the UGV is visiting, c is the total cost of the edges traversed
 340 so far and

341
$$n_i = \begin{cases} 0 & \text{if the node } a_i \text{ has not yet been visited} \\ 1 & \text{if the node } a_i \text{ has been visited} \\ 2 & \text{if the data associated with node } a_i \text{ has been transmitted} \\ 3 & \text{if the task required for the node } a_i \text{ has been performed} \end{cases}$$

342 **Definition 5.1.** *The state $\mathbb{S} = (n_1, n_2, \dots, n_A, u, c)$ is said to be a feasible so-*
 343 *lution of the problem if $u = s$ and*

344
$$n_i = 3 \quad \forall i \in \{1, 2, \dots, A\}$$

345 The state $\mathbb{S} = (n_1, n_2, \dots, n_A, u, c)$ is branched taking into consideration all
 346 possible displacements of the UGV from the node u to any other node connected
 347 to u by one edge and this leads to the construction of the state tree as illustrated
 348 in Example 5.1.

349 **Example 5.1.** *Consider the network in Fig. 1 in which the node $a_1 \in \mathcal{A} \setminus \mathcal{B}$,*
 350 *$a_2 b_2 \in \mathcal{A} \cap \mathcal{B}$, $s \in \mathcal{B}$ and $b_1 \in \mathcal{B}$. The network shows two nodes of interest*

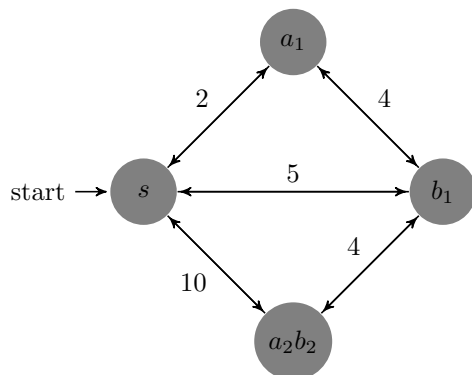


Figure 1: Network of the example 5.1

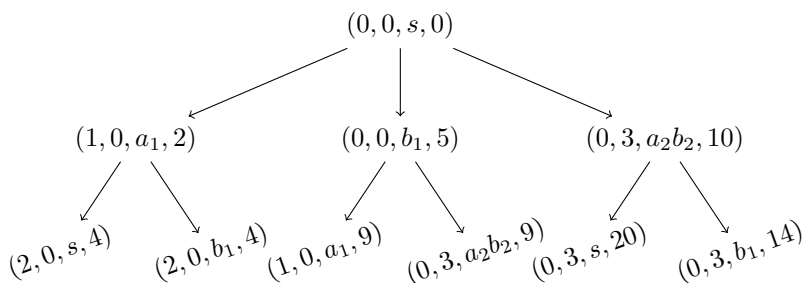


Figure 2: State tree of the example 5.1

351 a_1 and a_2b_2 and hence the generic state is given by (n_1, n_2, u, c) in which n_1
 352 and n_2 are associated with a_1 and a_2b_2 (see Eq. (5)) In Fig. 2 we represent
 353 part of the tree of the states that are generated by the algorithm. The root of
 354 the tree is the state $(0, 0, s, 0)$ corresponding to the initial location. From node
 355 s , if the UGV moves to the node a_1 , n_1 takes value 1 and the new state will
 356 be $(1, 0, a_1, 2)$; if the UGV moves to node b_1 , the new state will be $(0, 0, b_1, 5)$.
 357 Finally, if the UGV moves to node a_2b_2 , since communication is possible there,
 358 the UGV will send the corresponding information and then it will perform the
 359 required task. Hence n_3 will assume value 3 and the state will be $(0, 3, a_2b_2, 10)$.
 360 Such reasoning is applied recursively to all the newly generated states. Figure 2
 361 shows also the next expansion for the next level of the visit.

362 The algorithm implements two main operations: branch and bound. The

363 first one (branch) consists in expanding the state tree by generating new states
 364 from its leaves, as illustrated in Example 5.1, and the second one (bound) con-
 365 sists in reducing the state tree by means of a pruning procedure that terminates
 366 the visit on the leaves of the state tree that can not lead to the optimal solu-
 367 tion. The decision on what leaf can or can not lead to an optimal solution, i.e.
 368 pruning, is based on the following two rules:

- 369 1. If the lower bound associated with any state among those to be expanded
 370 (the leaves) is greater than the cost of any already computed feasible
 371 solution, such state is closed, i.e., it is no more considered for branching.
- 372 2. If any state among those to be branched differs from a state \mathbb{S} already
 373 reached just for its cost, such state is closed if its cost is greater than the
 374 one of \mathbb{S} .

375 In order to derive a lower bound associated with a state $\mathbb{S} = (n_1, n_2, \dots, n_A, u, c)$,
 376 first let us consider the set

$$377 \quad \mathcal{V}_{\mathbb{S}} = \{a \in \mathcal{A} \mid n_a \neq 3\}.$$

378 At the state \mathbb{S} , each node $a \in \mathcal{V}_{\mathbb{S}} \setminus \mathcal{B}$ such that $n_a = 0$ is still to be visited
 379 at least twice and those with $n_a = 1$ or $n_a = 2$ should still be visited at least
 380 once. Thus, in (34), each node $a \in \mathcal{V}_{\mathbb{S}} \setminus \mathcal{B}$ has still to be visited at least
 381 $2 - \min(n_a, 2)$ times. Furthermore, each node $b \in \mathcal{V}_{\mathbb{S}} \cap \mathcal{B}$ still has to be visited
 382 at least once. The information acquired in each node $a \in \mathcal{V}_{\mathbb{S}} \setminus \mathcal{B}$ has then
 383 to be transmitted by visiting some of the nodes $b \in \mathcal{B}$ and, finally, the UGV
 384 has to go back to the depot s . Since we are searching for a lower bound of
 385 the time needed to perform the aforementioned operations, we relax the flow
 386 conservation constraints, hence we assume that: i) the UGV visits and leaves
 387 each node $j \in \mathcal{V}_{\mathbb{S}}$ using the cheapest edge connected to it ($\min_{i \in \mathcal{V}} t_{ij}$); ii) the
 388 transmissions occurs only once at some node $b \in \mathcal{V}_{\mathbb{S}} \cap \mathcal{B}$ if there is any, otherwise
 389 it occurs at the node $b \in \mathcal{B}$ that is reachable from any node that is still to be
 390 visited assuming to spend the smallest possible time ($\min_{i \in \mathcal{V}_{\mathbb{S}}, j \in \mathcal{B}} t_{ij}$); iii) the
 391 UGV will go back to the depot using the lowest amount of time needed to reach

392 it from a node $i \in \mathcal{V}_\mathbb{S}$ ($\min_{i \in \mathcal{V}_\mathbb{S}} t_{is}$). Such relaxations clearly lead to a total time
 393 that is smaller than or equal to the time that is actually needed and hence any
 394 solution derived from the state \mathbb{S} is lower bounded by

$$\begin{aligned}
 395 \quad LB_\mathbb{S} = c + & \left(\sum_{a \in \mathcal{V}_\mathbb{S} \setminus \mathcal{B}} (2 - \min(n_a, 1)) \min_{i \in \mathcal{V}} t_{ia} \right) + \left(\sum_{b \in \mathcal{V}_\mathbb{S} \cap \mathcal{B}} \min_{i \in \mathcal{V}} t_{ib} \right) + \\
 & (1 - \min(1, |\mathcal{V}_\mathbb{S} \cap \mathcal{B}|)) * \min_{i \in \mathcal{V}_\mathbb{S}, j \in \mathcal{B}} t_{ij} + \min_{i \in \mathcal{V}_\mathbb{S}} t_{is}.
 \end{aligned} \tag{34}$$

396 It is worth noting that the lower bound proposed in (34) is not particu-
 397 larly complex nor computationally expensive. Therefore it can be considered
 398 a reasonably simple example of how the proposed algorithm can be improved.
 399 Nevertheless, the use of such lower bound can systematically reduce the time
 400 needed to find an optimal solution, as shown in Section 6.

401 Another example about how the proposed algorithm can be improved is to
 402 make available to the algorithm itself an initial feasible solution so that the
 403 lower bound can be effectively used right from the start. Such initial feasible
 404 solution is computed using a nearest neighbour algorithm that implements the
 405 steps in Algorithm 1.

Algorithm 1 Compute Initial Feasible Solution

- 1: run the Bellman Ford algorithm to find the shortest path between each pair
of nodes (i, j) , $j \in \mathcal{V}$, $i \in \mathcal{V}$ and its total cost c_{ij} ;
 - 2: $\mathcal{T} = \mathcal{A}$, $C=0$;
 - 3: find the node $\hat{a} \in \mathcal{T}$ such that $c_{s\hat{a}} = \min_{a \in \mathcal{A}} c_{sa}$ and set $C = C + c_{s\hat{a}}$
 - 4: $\mathcal{T} = \mathcal{T} \setminus \{\hat{a}\}$
 - 5: if $\mathcal{T} \neq \emptyset$, find the node $b \in \mathcal{T}$ such that $c_{\hat{a}b} = \min_{i \in \mathcal{T}} c_{\hat{a}i}$; set $C = C + c_{\hat{a}b}$,
let $\hat{a} = b$, go back to step 4.
 - 6: find the node $i \in \mathcal{B}$ such that $c_{\hat{a}i} = \min_{j \in \mathcal{B}} c_{\hat{a}j}$; set $C = C + c_{\hat{a}i}$
 - 7: $C = 2C$
 - 8: return C
-

406 The underlying idea is the following: starting from the depot s , the UGV
 407 chooses and visits the closest type A node (i.e., the one reachable in the lowest

408 possible amount of time); then, from that node, it selects the next node in the
 409 set of those to be visited using the same criteria; this process is repeated until
 410 all nodes of type A are visited. Then, a type B node is visited to transmit the
 411 acquired data. Finally, all the nodes are visited again following back the path
 412 used for data collection, i.e., the cost is doubled. Clearly, this is not the best
 413 solution, but it is a value that can be immediately compared with the computed
 414 lower bound also in the initial phases when a feasible solution would not be
 415 available otherwise.

416 Also, another important factor to consider in order to make the algorithm
 417 faster is that while expanding the state tree, leaves can be considered in several
 418 different orders by means of a priority value. The simplest strategy to assign
 419 such a value is to use a monotonically decreasing value each time a new leaf
 420 is created. In such a way leaves are considered in creation order. Other more
 421 advances strategies are possible and they will be presented and investigated in
 422 Section 6.

423 When branching a leaf \mathbb{S} , it may happen that all the states generated from \mathbb{S}
 424 are canceled when the two pruning rules are applied. In this case \mathbb{S} is closed and
 425 no more considered. Note that closed states also include feasible solutions which
 426 clearly do not need to be further expanded. The expansion of the state tree and
 427 the pruning procedure are then iteratively applied until all the leaves of the
 428 state tree are closed. In order to formally present the algorithm we introduce
 429 the following definitions:

- 430 • \mathcal{G} the graph associated with the problem;
- 431 • \mathcal{S}_T the state tree;
- 432 • N_U the number of nodes adjacent to node U in the graph \mathcal{G} ;
- 433 • \mathcal{L}_g the list of all new states generated when branching the leaf having
 434 highest priority;
- 435 • \mathcal{L}_p the list of all the states in \mathcal{L}_g that are not pruned after the function
 436 $Prune()$ has been called;

- 437 • \mathcal{F} the list containing the closed states;
- 438 • $\{\}$ the empty list
- 439 • $Pop(\mathcal{L})$ a function that takes as input a list of states and returns the state
440 \mathbb{S} with highest priority;
- 441 • $Branch(\mathbb{S}, \mathcal{G})$ a function that takes as input a state $\mathbb{S} = (n_1, n_2, \dots, n_A, U, C)$
442 and the graph, branches the received state and returns a list of N_U states,
443 one for each of the adjacent nodes to U (see Example 5.1);
- 444 • $Insert(\mathcal{L}_p, \mathcal{S}_T)$ a function that inserts in the state tree the list of states
445 received as input;
- 446 • $Prune(\mathcal{S}_T, \mathcal{L}_g)$ a function that takes as input the state tree \mathcal{S}_T and the
447 list of newly generated states \mathcal{L}_g then eventually prunes some states from
448 \mathcal{S}_T and \mathcal{L}_g according to the aforementioned pruning rules and returns the
449 list of remaining states from \mathcal{L}_g ;
- 450 • $GetSolution(\mathcal{S}_T)$ a function that extracts from the state tree the branch
451 that leads to the leaf state that is a feasible solution with the minimum
452 cost.

453 The algorithm consists of the steps defined in Algorithm 2.

454 It is worth noting that the proposed algorithm solves the problem *without*
455 *making any assumption* neither on the value of K nor on the number of dummy
456 vertices associated with each node. The value of K can be simply computed at
457 the end by just counting the number of displacements performed by the UGV.

Algorithm 2 Compute Optimal Path

```
 $\mathcal{S}_T = \{(0, 0, \dots, S, 0)\}$   
 $\mathcal{F} = \{\}$   
while  $(\mathbb{S} = \text{Pop}(\mathcal{S}_T \setminus \mathcal{F})) \neq \{\}$  do  
     $\mathcal{L}_g = \text{Branch}(\mathbb{S}, \mathcal{G})$   
     $\mathcal{L}_p = \text{Prune}(\mathcal{S}_T, \mathcal{L}_g)$   
    if  $(\mathcal{L}_p == \{\})$  then  
         $\mathcal{F} = \mathcal{F} \cup \mathbb{S}$   
    else  
         $\text{Insert}(\mathcal{L}_p, \mathcal{S}_T)$   
    end if  
end while  
 $\text{Sol} = \text{GetSolution}(\mathcal{S}_T)$ 
```

458 **6. Numerical results and discussion**

459 The numerical experiments conducted in this section aim at comparing the
460 complexity of solving the problems using both the integer and mixed integer
461 linear programming problems represented respectively by Model I and Model II
462 and our proposed algorithm.

463 Two sample graphs are shown respectively in Fig. 3 and Fig. 4. A different
464 labelling has been adopted for these graphs in order to make them more readable
465 when superimposed on a map. Here we use symbols instead of letters:

- 466 • the *squares* represent nodes of type *A*
- 467 • the *diamonds* represent nodes of type *B*
- 468 • the *stars* represent nodes of type *AB*

469 While Fig. 3 is a simple example drawn up from scratch, the graph in Fig. 4
470 represents a more realistic case that has been obtained by mapping a vineyard
471 of the Langhe area in Piedmont (Italy) on an undirected graph with 33 nodes
472 and 39 edges representing the paths across the 9 rows of the vineyard.

473 First, in order to quantify how the effectiveness and efficiency of Model I is
474 affected by the value of K , we first find the lowest value of K that yields the
475 optimal solution in Model I by running our branch and bound algorithm. Then,
476 Model I is solved by means of the integer linear programming solver available in
477 the CPLEX software [48] using different estimations of K including the previous
478 one. We remind that the number K of displacements of the UGV required to
479 perform all the tasks in the shortest possible time is dependent on the topology
480 of the considered graph. Choosing K according to (15) guarantees to find the
481 optimal solution. However, to explore the performance provided by commercial
482 solvers such as CPLEX, we tested different K values. To better quantify the
483 different amount of time required as a function of K , we propose to evaluate
484 the following ratio:

$$485 \rho = \frac{T_K}{T_{opt}}$$

486 where T_K and T_{opt} are the times required by CPLEX to solve the problem using
487 a certain value of K and the lowest K value that yields the optimal solution,
488 respectively. Table 1 presents the results obtained for the graph in Fig. 3.
489 The experiments have been performed using IBM ILOG CPLEX Optimization
490 Studio 12.9.0.0 on a Dell PowerEdge T640 with an Intel Xeon 4114 2.2 GHz 64
491 bit deca-core processor and 32 GB of DDR4 2400 MT/s memory. If K is less
492 than 18, i.e., the lowest value that allows to compute the optimal solution, the
493 CPLEX solver either finds a cost higher than the optimal one or no solution at
494 all. When $K = 18$, the CPLEX solver finds the optimal solution, as expected.
495 A rather small overestimation of K , e.g., $K = 22$ instead of $K = 18$, makes
496 CPLEX about 7 times slower, and even worse for higher values.

497 To present a more comprehensive set of results, we now focus our attention
498 on the topology in Fig. 4 which is far more complex than the one in Fig. 3. Due
499 to our interest in the agricultural application, this topology will be taken as
500 the basis to randomly generate many different graphs with a variable number
501 of nodes to visit and thus different complexity. In practice, starting from the
502 full graph, some of its type A nodes are transformed into “transit” nodes in

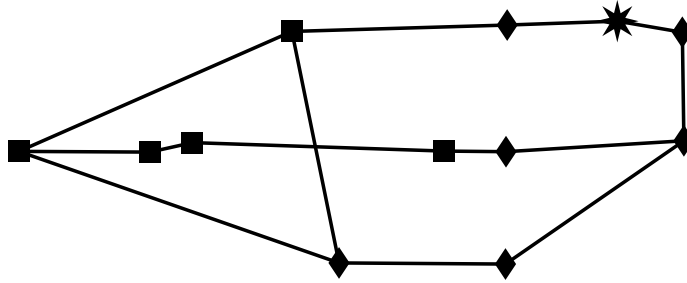


Figure 3: Sample graph drawn from scratch to mimic a possible field. Here the nodes represent: POIs that need to be visited (squares), places where it is possible to communicate (diamonds), or locations that are both (stars).

	K	T_K (s)	ρ	Cost
underestimation of the K value	10	2.16	0.12	–
	12	3.88	0.22	–
	15	6.17	0.36	100
K optimum value	18	17.33	1.00	94
overestimation of the K value	20	40.05	2.31	94
	22	120.01	6.92	94
	> 25	> 1000	> 57.70	94

Table 1: Time (T_K) taken by the CPLEX solver for the graph in Fig. 3 for different K values in Model I.

503 which the UGV must not perform any operation (they are neither of type A or
 504 B or AB). Also, in all experiments, the time required to cover an edge (t_{ij}) is
 505 directly proportional to the length of the edge itself.

506 More precisely, Table 2 and 3 report the time taken by CPLEX to find
 507 the optimal solution using Model I and Model II, for different combinations of
 508 number of labelled nodes N (hence the sum of A , B and AB nodes) and position
 509 of such nodes. When CPLEX exceeded the given time limit of two hours, we
 510 report a percentage in brackets (instead of the duration of the computation)
 511 that represents how much the best solution found by the model exceeds the



Figure 4: Undirected graph that represents the available paths for the UGV on a real vineyard. Nodes are marked as described in Fig. 3 and represent the type A, B, AB nodes with the addition of some “transit” nodes marked as empty circles.

512 optimal solution. Also, note that all the values shown in the tables have been
 513 obtained in the best possible conditions, i.e., when the value of K leading to
 514 the optimal solution is known (for Model I) and when the number of dummy
 515 vertices to use is known (for Model II).

516 The results in Table 2 and Table 3 show that Model II performs better than
 517 Model I almost all the times. For Model I the execution time is quite large and
 518 can exceed the given time limit also for relatively small graph instances. Both
 519 models, when interrupted after two hours of computation, are able to provide
 520 an intermediate best solution that in some cases is very close to the optimal
 521 one, but that tends to derive more and more for complex graph instances. Our
 522 proposal, instead, is always able to compute a solution in the given time limit

N	#1	#2	#3	#4	#5	#6	#7	#8	#9	#10
11	14.76	493.69	0.77	83.87	0.96	469.49	3.82	(7.30%)	(3.11%)	(1.02%)
12	2319.38	2.60	1647.31	4.35	1647.31	4.35	3.52	(7.30%)	(0.00%)	(2.18%)
13	7.61	40.61	4090.54	823.92	346.69	7.34	(7.47%)	(4.57%)	(0.54%)	(0.00%)
14	4670.32	18.86	856.01	(7.59%)	(0.61%)	(1.56%)	(8.47%)	(14.97%)	(3.39%)	(5.26%)
15	1723.71	2057.74	4100.92	429.9	(0.00%)	(0.00%)	(0.00%)	(14.33%)	(30.49%)	(5.72%)
16	2700.44	3920.32	(3.83%)	(3.38%)	(0.00%)	(7.02%)	(2.25%)	(11.34%)	(8.18%)	(6.87%)
17	(34.07%)	(3.33%)	(14.74%)	(38.41%)	(6.06%)	(35.94%)	(37.23%)	(27.65%)	(39.01%)	(53.03%)
18	(34.11%)	(8.96%)	(9.21%)	(25.69%)	(11.24%)	(28.14%)	(36.87%)	(55.70%)	(29.28%)	(18.50%)

Table 2: Time (s) required to solve Model I with a time limit of two hours. For each number of nodes N , ten problem instances (#1 ... #10) have been randomly generated. When the time limit has been reached we report, in brackets, how much the best solution found by the model exceeds the optimal one.

N	#1	#2	#3	#4	#5	#6	#7	#8	#9	#10
11	5.73	8.79	4.78	40.25	3.56	12.55	1.47	32.55	30.45	12.77
12	21.04	7.58	8.90	27.78	8.90	27.78	8.40	17.34	43.07	19.14
13	10.93	38.17	44.28	12.31	7.40	7.32	49.01	137.86	5.31	39.72
14	24.87	483.22	14.37	82.69	46.27	114.50	116.87	54.01	32.55	597.56
15	10.63	133.05	138.65	2570.43	234.08	770.36	97.99	217.67	532.98	1327.23
16	27.95	21.52	454.72	436.22	474.42	262.23	1757.05	1229.74	1237.98	(0.00%)
17	207.71	3261.04	626.26	1653.33	2485.79	(11.45%)	(18.56%)	(7.34%)	(22.15%)	(8.51%)
18	412.53	1058.85	2258.76	(11.02%)	(9.62%)	(12.41%)	(10.20%)	(12.41%)	(9.47%)	(22.74%)

Table 3: Time (s) required to solve Model II with a time limit of two hours. For each number of nodes N , the same ten instances of Table 2 have been used. When the time limit has been reached we report, in brackets, how much the best solution found by the model exceeds the optimal one.

523 and, when the CPLEX Model II is able to find a solution, performs 20 to 30
524 times faster than that.

525 Regarding our proposed algorithm, four cases have been considered. They
526 are named *normal*, *reduced*, *advanced*, and *lower bound* in the following. The
527 *normal* approach corresponds to the algorithm that runs on the graph as built
528 from the real sample vineyard shown in Fig. 4. In such a graph we have reported
529 also some additional nodes (marked as circles in the figure) to represent the path
530 of the UGV in the vineyard and not only the connections between the nodes
531 of type A , B , AB . We define such nodes as “transit” nodes because in our

532 algorithm, when such nodes are visited, the state remains unchanged except
533 for the cost of the path that is updated consequently. Clearly, introducing new
534 nodes into a graph increases the total number of nodes which has a direct impact
535 on the problem’s complexity.

536 Therefore, in order to minimize the complexity, the graph from Fig. 4 can be
537 reduced by producing an equivalent “reduced” graph that has less nodes because
538 all the nodes that are just transit nodes have been substituted by direct edges
539 between the adjacent nodes, so that the same topology is maintained but the
540 number of nodes is reduced. This is referred to as the *reduced* approach in the
541 latter, which always runs on the “reduced” graph version.

542 The *advanced* approach is similar to the *reduced* approach, i.e., it runs on
543 the “reduced” graph, but the priority value described in Section 5 has been
544 changed. The priority is set to the inverse of the cost of the state (named
545 *costonly* in the following) thus the state tree is always expanded from the leaf
546 state with the lower cost. Following the minimum cost path, and not a path
547 given by the ordering of the nodes, the pruning function is more efficient and a
548 larger number of states are discarded by the prune rules because the algorithm
549 already found an equivalent state with a lower cost.

550 Finally, the *lower bound* approach works as the *advanced* one but at each
551 new state it computes a lower bound, as previously described in Section 5, to
552 prune branches faster, hence to reduce execution time.

553 Results are reported in Table 4 as the average on 50 different random graphs,
554 for different numbers of nodes N . As it might be expected, the complexity scales
555 exponentially with the number of nodes to be visited (i.e., transmitted and re-
556 visited). However, the cost of finding the optimal solution is heavily reduced
557 if the *advanced* approach is employed. In fact, in the *reduced* approach, every
558 time a new node to be visited is added to the graph, the size of the state tree is
559 increased by a factor of 4.40, while in the *advanced* approach only by a factor
560 of 3.71. Here the S_T size corresponds to the number of nodes in the state
561 tree as defined in Section 5. This value equals the number of times the loop
562 in Algorithm 2 is run, thus it is directly proportional to the average execution

N	<i>normal</i>		<i>reduced</i>		<i>advanced</i>		<i>lower bound</i>	
	\mathcal{S}_T size	time	\mathcal{S}_T size	time	\mathcal{S}_T size	time	\mathcal{S}_T size	time
11	52529	3.0	5879	0.5	1121	0.1	852	0.1
12	258049	15.2	34623	3.7	4275	0.5	3222	0.4
13	979446	60.4	158299	16.8	16957	1.9	12842	1.7
14	4018175	267.7	715881	76.2	65044	8.1	45478	6.3
15	14663488	1014.4	2789828	279.7	245102	30.1	164629	21.8
16	55298726	4135.3	12438650	1308.6	988588	128.0	625578	86.7
17	-	-	57007645	5906.8	3631947	475.6	2866574	407.4
18	-	-	-	-	10687414	1388.2	7998251	1127.1

Table 4: Complexity of the various approaches, in terms of number of nodes in the state tree (\mathcal{S}_T size) and execution time (seconds). Each row reports the average on 50 different random instances, for different numbers of nodes N .

563 time, also shown in Table 4. Additional time reductions are possible if lower
564 bound techniques are used to prune states faster while exploring them, as done
565 by the *lower bound* approach, or if an initial feasible solution is provided right at
566 the start of the algorithm. While the lower bound consistently allows to reduce
567 the computation time with all the instances, the initial solution does not always
568 provide a significant gain because the priority used to visit the nodes is already
569 based on a minimum cost criterion.

570 To better visualize the data, we also plot the time (on a logarithmic scale) as
571 a function of N in Figure 5. It is clear that the best approach is the *lower bound*
572 one, which can consistently outperform the others, keeping approximately the
573 same distance from the *advanced* one in terms of relative time reduction, which
574 is about 20%. We did not test graphs with more than $N = 18$ because in
575 that case also our algorithm would have rapidly exceeded the two hours time
576 bound we used for the experiments. In fact, the exponential trend at which the
577 computation time increases can be clearly deduced from Figure 5.

578 Table 5 shows the individual times required by the best variant (*lower bound*)

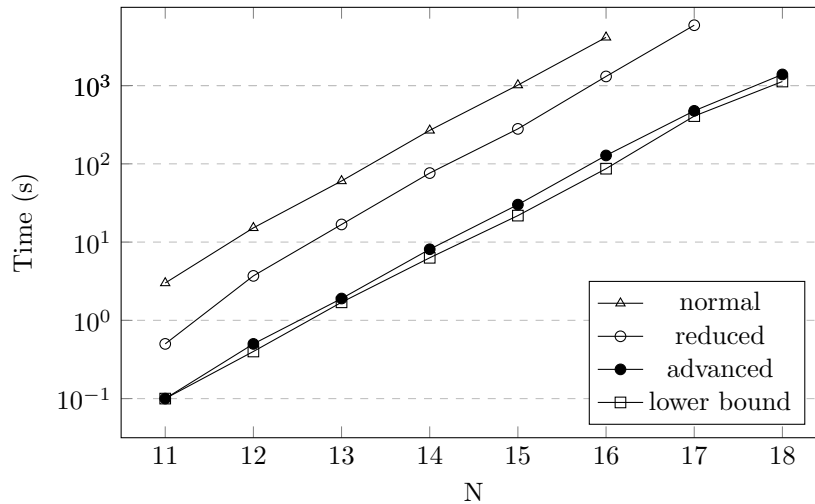


Figure 5: Time required by the different approaches of our proposed algorithm, as a function of the number of nodes N .

579 of our proposed algorithm for each number of nodes N , on the same ten different
 580 randomly generated graphs as in Table 2 and 3. It is clear that our algorithm
 581 provides lower execution time. Moreover, it does not require to estimate any
 582 other parameter to be fed as input as it happens for Model I and Model II.
 583 Despite the execution time of the ILP formulations can, occasionally, be some-
 584 how close to the one of our algorithm, Table 5 clearly shows that our algorithm
 585 exhibits much more consistency across different problem instances, which is not
 586 the case for the ILP formulations. For example, the CPLEX solver using Model
 587 II happens to exceed the given two hours time bound starting from $N = 16$
 588 and at more than half of the times for the more complex graph instances. For
 589 the less complex instances we computed that, on average (over the 50 tested
 590 instances), our proposed algorithm is about 20 to 30 times faster as it can be
 591 seen also by comparing the results for the few instances presented in Table 3
 592 and 5.

593 Note also that our algorithm has been implemented, to speed up develop-
 594 ment, in the *python* scripting language, which is not particularly optimized for
 595 speed. Therefore the shown time difference could potentially be improved by

N	#1	#2	#3	#4	#5	#6	#7	#8	#9	#10
11	0.09	0.12	0.09	0.06	0.10	0.07	0.08	0.11	0.11	0.12
12	0.38	0.37	0.45	0.46	0.45	0.46	0.36	0.42	0.48	0.48
13	1.25	1.07	1.65	2.03	1.88	1.54	1.41	1.82	2.36	2.19
14	6.94	7.67	6.73	8.13	5.09	7.41	6.42	9.97	6.43	4.60
15	21.65	16.52	17.45	22.96	19.00	21.05	17.31	22.87	29.73	29.83
16	83.43	66.34	82.52	107.13	114.55	76.65	81.24	94.96	76.73	86.66
17	411.03	507.35	352.81	328.25	391.64	446.76	409.63	303.40	404.87	449.02
18	1057.29	1067.60	905.80	1374.41	1371.11	1432.13	872.12	1200.19	1232.31	1054.64

Table 5: Time (s) required to solve the problem using the best variant of the proposed algorithm (with lower bounds). For each number of nodes N, the same ten instances of Table 2 have been used.

rewriting our algorithm in native code.

Note that in this work we always focused on finding the guaranteed optimal solution to the problem. In fact, also with the *advanced* and *lower bound* approaches, the optimality of the solution is preserved.

In order to present a more comprehensive view of the algorithm, we also investigated how fast the algorithm converges towards the optimal solution. Therefore, knowing the cost value of the optimal solution, we plotted how far is the current solution at each step of the algorithm with respect to the optimal one. We compared two different priority functions, i.e., the *costonly* one which has just been described, and the *mixed* one where the priority is defined as follows

$$\pi_{\mathbb{S}} = \frac{\frac{1}{3A} \sum_{i=1}^A n_i}{c} \quad (35)$$

where the state is $\mathbb{S} = (n_1, n_2, \dots, n_A, u, c)$. The basic idea is that the numerator in (35) provides an estimation of how close a state is from a feasible solution. In fact, considering that n_i can assume increasing values, from 0 (the initial state) to 3 (the final state), the higher the value of the sum, the more the visit is near to its completion. The $\frac{1}{3A}$ coefficient normalizes the numerator for the feasible

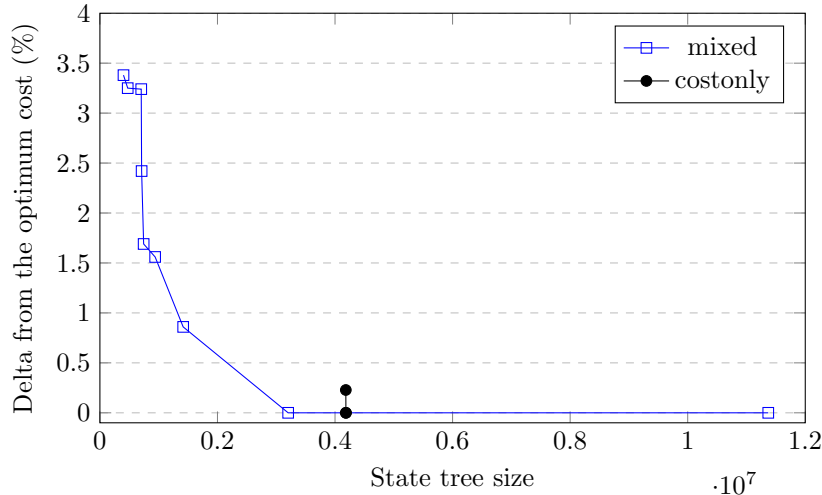


Figure 6: Analysis of the optimality of the intermediate solutions found using two different priority measures. The *costonly* measure terminates earlier with a small total state tree size, but finds a feasible solution only at the very end of the execution. The *mixed* measure makes the algorithm move faster towards a (suboptimal) feasible solution, but delays its completion.

612 solution to 1, since n_i ranges from 0 to 3. If the next leaf to be branched is
 613 chosen according to (35), it is expected to reach a (somewhat “good”) feasible
 614 solution faster than in the case we use the *costonly* priority measure. That is
 615 because the priority value defined in (35) takes in consideration both how much
 616 of the visit has already been completed and how much it costs, thus it may tend
 617 to favour a path that completes faster the visit of the nodes, than just a path
 618 with the minimum cost.

619 Figure 6 shows that, for the priority function in (35), with less than 1/10
 620 of the size of the fully grown state tree, the current solution differs from the
 621 optimal one only for less than 3.5%. This is an encouraging result to be explored
 622 in future work where more efficient heuristics could be investigated.

623 7. Conclusions

624 In this work we proposed an algorithm to solve the navigation problem of a
 625 UGV that aims to minimize the time needed to perform repeated acquisition,

626 communication and action tasks on a predetermined set of positions. Starting
627 from the graph, we proposed both a modeling approach based on integer linear
628 programming, to be tackled through commercial solvers, and a branch and
629 bound algorithm specifically designed for the problem. The algorithm has been
630 explained in details by means of detailed pseudocode and examples. Results
631 showed that the proposed algorithm is able to provide an improvement of 20 to
632 30 times over commercial linear programming solvers when compared on many
633 instances that can be solved to optimality in reasonable computational time.
634 Tests have been conducted on both synthetically generated input data and data
635 extracted from a real world case. Moreover, faster variants of the algorithm
636 have also been proposed while solution optimality is maintained. While our
637 proposals can help to speed up computation compared to the ILP approach,
638 the complexity still increases exponentially with the number of nodes due to
639 the nature of the problem. Therefore, future work will be devoted to investigate
640 efficient heuristics able to find good solutions with acceptable response times,
641 maybe even able to run on the robots themselves. As a first step in this direction,
642 in this work we also investigated how fast the proposed algorithm converges to
643 the optimal solution, providing an insight into how it is possible to extend this
644 work by designing efficient heuristics.

645 **8. Acknowledgements**

646 This work has been supported in part by the Politecnico di Torino Interde-
647 partmental Center for Service Robotics (PIC4SeR) <https://pic4ser.polito.it>.

648 **9. References**

649 **References**

- 650 [1] C. Zecha, J. Link, W. Claupein, Mobile sensor platforms: Categorisation
651 and research applications in precision farming, *Journal of Sensors and Sen-
652 sor Systems* 2 (1) (2013) 51–72.

- 653 [2] S. Bonadies, A. Lefcourt, S. A. Gadsden, A survey of unmanned ground
654 vehicles with applications to agricultural and environmental sensing, in:
655 Autonomous Air and Ground Sensing Systems for Agricultural Optimiza-
656 tion and Phenotyping, Vol. 9866, International Society for Optics and Pho-
657 tonics, 2016, p. 98660Q.
- 658 [3] S. Candiago, F. Remondino, M. De Giglio, M. Dubbini, M. Gattelli, Eval-
659 uating multispectral images and vegetation indices for precision farming
660 applications from UAV images, *Remote Sensing* 7 (4) (2015) 4026–4047.
- 661 [4] V. Lukas, J. Novák, L. Neudert, I. Svobodova, F. Rodriguez-Moreno,
662 M. Edrees, J. Kren, The combination of UAV survey and landsat imagery
663 for monitoring of crop vigor in precision agriculture, *ISPRS-International*
664 *Archives of the Photogrammetry, Remote Sensing and Spatial Information*
665 *Sciences* 41 (2016) 953–957.
- 666 [5] Q. Vu, M. Raković, V. Delic, A. Ronzhin, Trends in development of UAV-
667 UGV cooperation approaches in precision agriculture, in: A. Ronzhin,
668 G. Rigoll, R. Meshcheryakov (Eds.), *Interactive Collaborative Robotics*,
669 Springer International Publishing, Cham, 2018, pp. 213–221.
- 670 [6] A. Vasudevan, D. A. Kumar, N. Bhuvaneshwari, Precision farming using
671 unmanned aerial and ground vehicles, in: *Technological Innovations in ICT*
672 *for Agriculture and Rural Development (TIAR)*, IEEE, 2016, pp. 146–150.
- 673 [7] A. Bechar, C. Vigneault, Agricultural robots for field operations: Concepts
674 and components, *Biosystems Engineering* 149 (2016) 94 – 111.
- 675 [8] S. Nandi, S. Thota, A. Nag, S. Divyasukhananda, P. Goswami, A. Aravin-
676 dakshan, R. Rodriguez, B. Mukherjee, Computing for rural empowerment:
677 enabled by last-mile telecommunications, *IEEE Communications Magazine*
678 54 (6) (2016) 102–109.
- 679 [9] G. R. MacCartney, Jr., S. Sun, T. S. Rappaport, Y. Xing, H. Yan, J. Koka,
680 R. Wang, D. Yu, Millimeter wave wireless communications: New results

- 681 for rural connectivity, in: Proceedings of the 5th Workshop on All Things
682 Cellular: Operations, Applications and Challenges, ATC '16, ACM, New
683 York, NY, USA, 2016, pp. 31–36.
- 684 [10] L. Fotio Tiotsop, A. Servetti, E. Masala, Optimally scheduling complex
685 logistics operations involving acquisition, elaboration and action tasks, in:
686 Proceedings of the 5th International Forum on Research and Technologies
687 for Society and Industry (RTSI), Florence, Italy, 2019, to be published.
- 688 [11] A. Castellini, A. Farinelli, G. Minuto, D. Quaglia, I. Secco, F. Tinivella,
689 EXPO-AGRI: Smart automatic greenhouse control, in: IEEE Biomedical
690 Circuits and Systems Conference (BioCAS), 2017, pp. 1–4.
- 691 [12] J. Dong, J. G. Burnham, B. Boots, G. Rains, F. Dellaert, 4D crop moni-
692 toring: Spatio-temporal reconstruction for agriculture, in: 2017 IEEE In-
693 ternational Conference on Robotics and Automation (ICRA), IEEE, 2017,
694 pp. 3878–3885.
- 695 [13] A. Chang, J. Jung, M. M. Maeda, J. Landivar, Crop height monitoring
696 with digital imagery from unmanned aerial system (UAS), *Computers and
697 Electronics in Agriculture* 141 (2017) 232–237.
- 698 [14] S. Khanal, J. Fulton, S. Shearer, An overview of current and potential
699 applications of thermal remote sensing in precision agriculture, *Computers
700 and Electronics in Agriculture* 139 (2017) 22–32.
- 701 [15] L. Comba, P. Gay, J. Primicerio, D. R. Aimonino, Vineyard detection from
702 unmanned aerial systems images, *Computers and Electronics in Agriculture*
703 114 (2015) 78–87.
- 704 [16] J. Primicerio, G. Caruso, L. Comba, A. Crisci, P. Gay, S. Guidoni, L. Gen-
705 esio, D. Ricauda Aimonino, F. P. Vaccari, Individual plant definition and
706 missing plant characterization in vineyards from high-resolution UAV im-
707 agery, *European Journal of Remote Sensing* 50 (1) (2017) 179–186.

- 708 [17] A. Matese, S. F. Di Gennaro, Technology in precision viticulture: A state
709 of the art review, *International Journal of Wine Research* 7 (2015) 69–81.
- 710 [18] J. Das, G. Cross, C. Qu, A. Makineni, P. Tokekar, Y. Mulgaonkar, V. Ku-
711 mar, Devices, systems, and methods for automated monitoring enabling
712 precision agriculture, in: *IEEE International Conference on Automation
713 Science and Engineering (CASE)*, IEEE, 2015, pp. 462–469.
- 714 [19] W. Pei, Y. Lan, L. Xiwen, Z. Zhiyan, Z. Wang, Y. Wang, Integrated sensor
715 system for monitoring rice growth conditions based on unmanned ground
716 vehicle system, *International Journal of Agricultural and Biological Engi-
717 neering* 7 (2) (2014) 75.
- 718 [20] Y. Marinakis, A. Migdalias, P. M. Pardalos, A new bilevel formulation for
719 the vehicle routing problem and a solution method using a genetic algo-
720 rithm, *Journal of Global Optimization* 38 (4) (2007) 555–580.
- 721 [21] Z. Huang, Q. P. Zheng, E. Pasilio, V. Boginski, T. Zhang, A cutting plane
722 method for risk-constrained traveling salesman problem with random arc
723 costs, *Journal of Global Optimization* (Sep 2018).
- 724 [22] E. Fadda, R. Tadei, G. Perboli, L. F. Tiotsop, The multi-path traveling
725 salesman problem with dependent random cost oscillations, in: *Seventh
726 Intl. Workshop on Freight Transportation and Logistics (ODYSSEUS)*,
727 Cagliari, Italy, 2018, pp. 368–371.
- 728 [23] G. Laporte, The vehicle routing problem: An overview of exact and ap-
729 proximate algorithms, *European Journal of Operational Research* 59 (1992)
730 345–358.
- 731 [24] B. Eksioglu, A. Volkan. Vural, A. Reisman, The vehicle routing problem:
732 A taxonomic review, *Computers & Industrial Engineering* 57 (2009) 1472–
733 1483.

- 734 [25] M. Salavati-Khoshghalb, M. Gendreau, O. Jabali, W. Rei, A hybrid re-
735 course policy for the vehicle routing problem with stochastic demands,
736 EURO Journal on Transportation and Logistics (2017) 1–30.
- 737 [26] H. Seyyedhasani, J. S. Dvorak, Using the vehicle routing problem to reduce
738 field completion times with multiple machines, Computers and Electronics
739 in Agriculture 134 (2017) 142 – 150.
- 740 [27] H. Seyyedhasani, J. S. Dvorak, Dynamic rerouting of a fleet of vehicles in
741 agricultural operations through a dynamic multiple depot vehicle routing
742 problem representation, Biosystems Engineering 171 (2018) 63 – 77.
- 743 [28] D. Bochtis, C. Sørensen, The vehicle routing problem in field logistics: Part
744 II, Biosystems Engineering 105 (2) (2010) 180 – 188.
- 745 [29] K. Zhou, A. L. Jensen, C. Sørensen, P. Busato, D. Bohtis, Agricultural
746 operations planning in fields with multiple obstacle areas, Computers and
747 Electronics in Agriculture 109 (2014) 12 – 22.
- 748 [30] M. Schiffer, M. Schneider, G. Walther, G. Laporte, Vehicle routing and
749 location routing with intermediate stops: A review, Transportation Science
750 53 (2) (2019) 319–343.
- 751 [31] B. Crevier, J.-F. Cordeau, G. Laporte, The multi-depot vehicle routing
752 problem with inter-depot routes, European Journal of Operational Re-
753 search 176 (2) (2007) 756–773.
- 754 [32] B.-I. Kim, S. Kim, S. Sahoo, Waste collection vehicle routing problem with
755 time windows, Computers & Operations Research 33 (12) (2006) 3624–
756 3642.
- 757 [33] T. Boussonville, A. Hartmann, T. Melo, H. Kopfer, Vehicle routing and
758 refueling: the impact of price variations on tour length, in: Logistikman-
759 agement, University of Bamberg Press, 2011, pp. 83–101.

- 760 [34] M. Schiffer, G. Walther, The electric location routing problem with time
761 windows and partial recharging, *European Journal of Operational Research*
762 260 (3) (2017) 995–1013.
- 763 [35] P. Vansteenwegen, W. Souffriau, K. Sörensen, The travelling salesperson
764 problem with hotel selection, *Journal of the Operational Research Society*
765 63 (2012) 207–217.
- 766 [36] M. Drexl, Synchronization in vehicle routing—a survey of VRPs with multi-
767 ple synchronization constraints, *Transportation Science* 46 (3) (2012) 297–
768 316.
- 769 [37] A. Gasparetto, P. Boscariol, A. Lanzutti, R. Vidoni, Path planning and tra-
770 jectory planning algorithms: A general overview, in: *Motion and operation*
771 *planning of robotic systems*, Springer, 2015, pp. 3–27.
- 772 [38] L. C. Basaca-Preciado, O. Y. Sergiyenko, J. C. Rodríguez-Quinonez,
773 X. Garcia, V. V. Tyrsa, M. Rivas-Lopez, D. Hernandez-Balbuena, P. Mer-
774 corelli, M. Podrygalo, A. Gurko, I. Tabakova, O. Starostenko, Optical 3D
775 laser measurement system for navigation of autonomous mobile robot, *Op-
776 tics and Lasers in Engineering* 54 (2014) 159–169.
- 777 [39] K. Ferentinos, K. Arvanitis, N. Sigrimis, Heuristic optimization methods
778 for motion planning of autonomous agricultural vehicles, *Journal of Global*
779 *Optimization* 23 (2) (2002) 155–170.
- 780 [40] O. Contente, N. Lau, F. Morgado, R. Morais, A path planning application
781 for a mountain vineyard autonomous robot, in: *Robot 2015: Second Iberian*
782 *Robotics Conference*, Springer, 2016, pp. 347–358.
- 783 [41] H. Zhang, W. Tong, Y. Xu, G. Lin, The Steiner traveling salesman problem
784 with online advanced edge blockages, *Computers & Operations Research*
785 70 (2016) 26 – 38.
- 786 [42] F. Nex, F. Remondino, UAV for 3D mapping applications: a review, *Ap-
787 plied geomatics* 6 (1) (2014) 1–15.

- 788 [43] J. Torres-Sánchez, J. M. Peña, A. I. de Castro, F. López-Granados, Multi-
789 temporal mapping of the vegetation fraction in early-season wheat fields
790 using images from UAV, *Computers and Electronics in Agriculture* 103
791 (2014) 104–113.
- 792 [44] G. Sona, D. Passoni, L. Pinto, D. Pagliari, D. Masseroni, B. Ortuani,
793 A. Facchi, UAV multispectral survey to map soil and crop for precision
794 farming applications, *International Archives of the Photogrammetry, Re-
795 mote Sensing and Spatial Information Sciences* 41 (2016) 1023–1029.
- 796 [45] J. Primicerio, G. Caruso, L. Comba, A. Crisci, P. Gay, S. Guidoni, L. Gen-
797 esio, D. Ricauda Aimonino, F. P. Vaccari, Individual plant definition and
798 missing plant characterization in vineyards from high-resolution UAV im-
799 agery, *European Journal of Remote Sensing* 50 (1) (2017) 179–186.
- 800 [46] W. E. Wilhelm, A technical review of column generation in integer pro-
801 gramming, *Optimization and Engineering* 2 (2) (2001) 159–200.
- 802 [47] Y. Zhao, T. Larsson, E. Rönnberg, P. M. Pardalos, The fixed charge trans-
803 portation problem: a strong formulation based on lagrangian decomposi-
804 tion and column generation, *Journal of Global Optimization* 72 (3) (2018)
805 517–538.
- 806 [48] IBM, CPLEX.
807 URL <https://www.ibm.com/products/ilog-cplex-optimization-studio>